FLOMEKO2019
18th International Flow Measurement Conference
Portugal | Lisbon | LNEC | 26-28 june 2019

Performance of the LDA Volumetric Flow Rate Standard Under Severely Disturbed Flow Conditions

Felix Heitmann[1], Jonas Steinbock and Markus Juling[1]

[1]*Physikalisch-Technische Bundesanstalt, Abbestraße 2-12, 10587 Berlin, Germany*
felix.heitmann@ptb.de

Abstract

In thermal power plants, flow meters are operated at high temperatures and pressures and often encounter disturbed flow profiles. This leads to an increased measurement uncertainty, which limits the save operating range of flow rates and hence the plant's power output. Therefore, the laser optical flow rate standard (LFS) was developed. It is designed to allow the on-site calibration of industrial flow meters in power plants at high temperatures and pressures. It makes use of the metrologically traceable and non-invasive laser Doppler anemometry (LDA) to measure the velocity field simultaneously with two LDA systems. The volumetric flow rate is then determined by means of integration. Here, we present flow rate measurements for fully developed pipe flow and 6 pipe diameters downstream of a disturbance generator. The mean deviation in flow rate between the two LDA systems was 0.05 %, with a mean deviation from the gravimetrical reference flow rate of 0.12 %. The highest deviations from the reference were 0.21 % and 0.31 %, for the two systems respectively.

1. Introduction

Industrial liquid flow rate meters are calibrated at test facilities which provide fully developed turbulent pipe flow, temperatures well below 100 °C and moderate pressures [1][2].
In contrast, water flow meters in power plants are operated at up to 400 °C and 300 bar.
Here, the fluid dynamic properties of water change drastically.
Further, the flow meter is deformed by the resulting thermal expansion and mechanical stress, changing the effective cross-sectional area.
Depending on the measurement principle, elevated temperatures will also affect the performance of the measurement equipment itself.
Due to space constraints, flow meters are often installed close to pipe bends and other instrumentation. This causes disturbed flow conditions inside the flow meters, resulting in deviations in the measured flow rate.

These factors aggregate to a measurement uncertainty in the field of around 2 % [3]. For operational safety, this limits the permissible range of flow rate and therefore the power output of the plant.

If the flow meters were to be calibrated in-situ, the factors mentioned above would be captured in the calibration process and therefore not be considered when determining the measurement uncertainty.
This, in turn, would lead to a major decrease in uncertainty of the flow rate and therefore allow the increase of the plant's power output.

A laser optical flow rate standard for high pressure natural gas was described by Mickan et al. [4]. The vastly different physical properties of water, however, require a very different design in many aspects.
LDA measurements for the determination of the flow rate in water were carried out by Müller et al. [5]. Yet, the design of the measurement setup prohibits the application at high temperatures and does not allow precise alignment of the LDA probe.

Thus, at the Physikalisch-Technische Bundesanstalt (PTB), a portable laser optical flow rate standard (LFS) was developed [3][6][7]. It employs the non-invasive and traceable laser-Doppler anemometry (LDA) for the point-wise measurement of the streamwise velocity. The flow field is approximated by spline (radial) and nearest-neighbor (azimuthal) interpolation between the measured points. The volumetric flow rate is determined by integration of the flow field over the pipe's cross-sectional area.

In this contribution, following a brief description of the LFS measurement setup, we present volumetric flow rate measurements obtained with the LFS under heavily disturbed flow conditions and compare them to the undisturbed, fully developed turbulent flow case.

2. Experimental setup

2.1 Configuration of the LFS
Optical access to the flow is provided by an industrial stainless-steel sight glass fitting (DN 150, PN 40) equipped with two metal fused sight glasses (PN 40, T_{max} = 280 °C) on opposing sides perpendicular to the direction of flow.
A short stainless-steel Venturi nozzle is installed inside the fitting, reducing the inner diameter from D_p = 158 mm at the inlet to 75 mm. This quadruples the mean velocity and therefore greatly increases the obtainable LDA burst rate. Furthermore, the flow profile is flattened considerably as described by Steinbock et al. [8].
Downstream of the nozzle, a calibrated precision glass pipe (r = (37.518 ± 0.008) mm) provides a well-defined cross section for the LDA measurements.

Pointwise velocity measurements are carried out simultaneously and independently by two cross beam LDA probes (P = 200 mW) with wavelengths of 532 nm and 561 nm, respectively.
In water, the resulting measuring volume is approximately 920 µm in length with a diameter of 65 µm (1/e²-criterion).
Each probe contains receiving optics that connect to a photomultiplier by multimode fiber optics.
As the two LDA probes are located on opposite sides of the optical access, each probe collects the forward scattered light from the other probe's measuring volume. This increases the obtainable LDA burst rate by a factor of 10 compared to operation in backward scattering mode.
The photomultiplier voltages are read out with a 12-bit digitizer and at least 10-fold oversampling of the LDA burst frequency.

The LDA probes are each mounted on a 6-axis hexapod positioning system. Besides traversing the LDA measuring volume over the pipe cross-section, they allow the precise alignment of the LDA probes to the glass pipe. A circumferential marking on the outer mantle of the glass pipe serves as a measurable reference of the pipe axis [3][9].

As the positioning system is not connected to the optical access pipe fitting, the alignment procedure is carried out before every measurement campaign. This physical separation between the potentially hot optical access and the positioning system allows the LFS to be used at high temperatures as the measurement systems is sensitive to temperature change.

When passing through the curved geometry of the glass pipe, the laser beams get refracted due to the difference in refractive indices. To place the measuring volumes at the desired positions inside the flow, numerical raytracing of the laser beams is performed individually for each positioning system and measuring position as described by Steinbock [6].

LDA measurements spanning the whole cross-section of the glass pipe are carried out at n_{rad} = 20 radial paths each containing 15 points between the pipe center and 0.99r (300 points in total). Hence, the last point is located at 375 µm distance from the wall. Between the pipe center and 0.8r, points are evenly placed at distances of 0.1r. Beyond 0.8r, 6 additional points are placed to minimize the error of the flow field integral [6].
This fine measurement grid allows the reconstruction even of strongly disturbed flow profiles and thereby the volumetric flow rate as later demonstrated.
Per point, LDA bursts are recorded until either a statistical uncertainty for the velocity of 0.05 % (k = 1) or a measurement time of 45 s is reached.

2.2 Data processing
For the near-wall positions, where the measuring volume partially intersects with the wall, the effective position is calculated as the intensity centroid of the remaining measuring volume according to Steinbock et al. [10].

To correct for the LDA velocity bias, the n individual burst velocities w_i of each measurement point (MP) are weighted with their respective inverse velocity according to Equation 1 and 2 as proposed by McLaughlin and Tiederman [11]. This seems to be adequate because the measured streamwise velocity is dominant over the other velocity components in this setup.

$$\overline{w}_{\mathrm{MP}} = \frac{\sum_{\mathrm{i}=1}^{n} w_{\mathrm{i}} * \xi_{\mathrm{i}}}{\sum_{\mathrm{i}=1}^{n} \xi_{\mathrm{i}}} \qquad (1)$$

$$\xi_{\mathrm{i}} = |w_{\mathrm{i}}|^{-1} \qquad (2)$$

For each radial path, a cubic Hermite spline is used to approximate the flow profile between the measured points. From the outermost point to the wall, the velocity profile is completed by the logarithmic law of the wall and a linear approach for the viscous sublayer.
As the wall shear stress is unknown, it is chosen so that the law of the wall velocity profile connects to the last measured point.

The volumetric flow rate is then calculated according to Equation (3).

$$Q_{\mathrm{LDA}} = \frac{2\pi}{n_{\mathrm{rad}}} \sum_{\mathrm{k}=1}^{n_{\mathrm{rad}}} \int_{0}^{r} w_{\mathrm{k}}(r)\, r\, dr \qquad (3)$$

Here, $w_{\mathrm{k}}(r)$ is the reconstruction of the velocity profile for the path k as a function of the radius r which is integrated analytically.

2.3 Flow facility and test bench setup
All measurements were conducted at the heat water calibration rig at the Physikalisch-Technische Bundesanstalt in Berlin [2] at p = 2.5 bar.
Using the gravimetrical principle, it exhibits a measurement uncertainty of U = 0.04 % (k = 2) for volumetric flow rates of water between 3 and 1000 m³/h and temperatures from 3 to 90 °C.

At first, the test bench was equipped with a straight DN 150 pipe (D_{p} = 158 mm) with a length of 50D_{p} upstream and 10D_{p} downstream of the LFS optical access for the measurement in fully developed pipe flow.
Afterwards, an asymmetrical swirl disturbance generator was inserted into the piping at 6D_{p} upstream of the LFS (see Figure 1).

The asymmetrical swirl disturbance generator as proposed by Tawackolian [12] features five angled blades and a disturbance plate blocking 7 % of the cross-sectional area. It was designed to emulate the flow pattern downstream of a double bend out of plane [12].
Further investigation of the resulting flow profile is described by Turiso et al. [13].

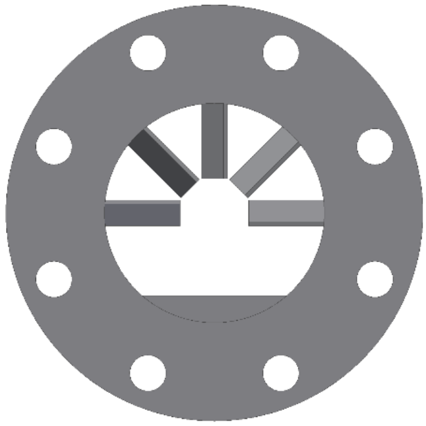

Figure 1: The DN 150 asymmetrical swirl disturbance generator in a DIN flange style.

For both configurations, measurements were carried out at 5 combinations of Reynolds numbers and temperatures (test cases) as shown in Table (1). For each measurement, a gravimetrical flow rate measurement Q_{ref} was performed.

All Reynolds numbers are stated with respect to the DN 150 pipe upstream of the LFS as given by

$$Re = \frac{w_{\mathrm{p}} D_{\mathrm{p}}}{\nu} \qquad (4)$$

and

$$w_{\mathrm{p}} = \frac{Q_{\mathrm{ref}}}{\frac{\pi}{4} D_{\mathrm{p}}^2}. \qquad (5)$$

Flow rate measurements were repeated 3 times for each configuration and test case.

Table 1: Flow parameters of the 5 test cases.

Test case	T (°C)	Re (10^3)	Q_{ref} (m³/h)
1	20	50	22.40
2	20	100	44.80
3	20	450	200.00
4	60	450	95.29
5	60	945	200.00

3. Results and discussion

In the following section, the two measurement systems are referred to as LDA1 (532 nm wavelength) and LDA2 (561 nm).

A single measurement of the volumetric flow rate took between 1.4 and 2 hours, with longer durations at low Reynolds numbers.

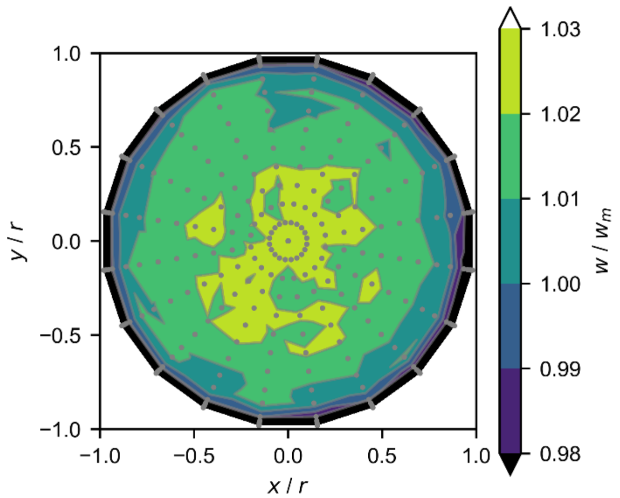

Figure 2: Normalized velocities of LDA2 at *Re* = 945*10³ and 60 °C for the undisturbed configuration.

To illustrate the flattening effect of the Venturi nozzle, Figure 2 shows the velocities measured with LDA2 under the undisturbed configuration at *Re* = 945*10³ and 60 °C, normalized by the mean velocity

$$w_{\mathrm{m}} = \frac{Q_{\mathrm{LDA}}}{\pi r^2}. \qquad (6)$$

Note that one shade of color represents velocities within a 1 % range. In the pipe center, the velocity exceeded the mean velocity by less than 3 %. Towards the pipe wall, the measured velocities stayed above w_{m} until around 0.95*r*.

A fully developed turbulent flow in the same diameter and smooth walls would show a much higher center velocity of around 1.16w_{m} and velocities lower than w_{m} as soon as 0.75*r*.

As the LDA burst frequency is proportional to the velocity, the bandwidth of the raw LDA signal encountered across most of the flow field of the LFS is much narrower than in a fully developed turbulent flow. This greatly facilitates the selection of appropriate filters.

Spatial fluctuations of the velocity of less than 1 % are visible. These might be caused by imperfections that were observed on the glass pipe surface.
In Figure 3, the normalized velocity profile of LDA2 is shown for the disturbed configuration at identical flow parameters as in Figure 2.

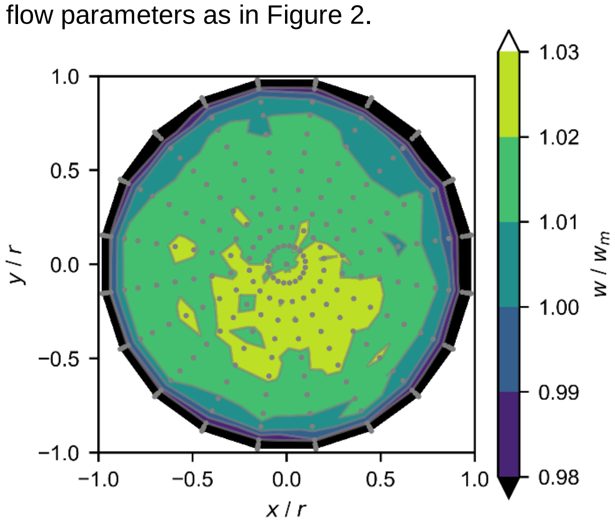

Figure 3: Normalized velocities of LDA2 at *Re* = 945*10³ and 60 °C for the disturbed configuration.

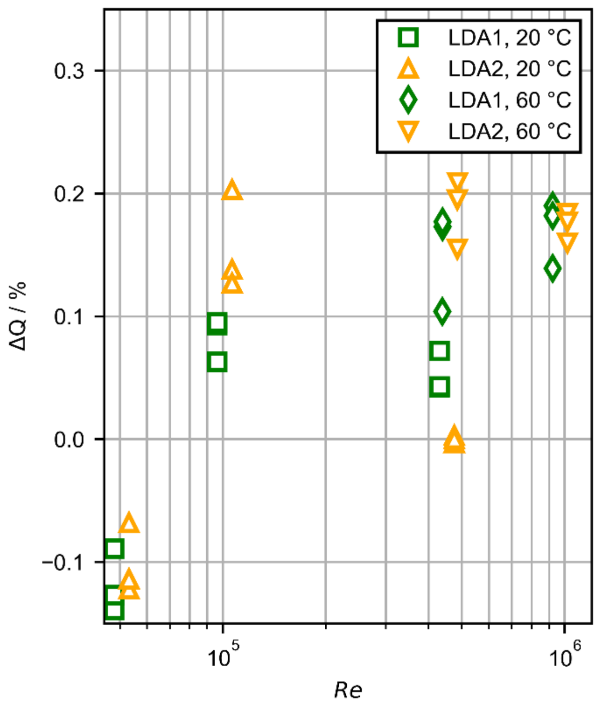

Figure 4: Relative deviations of the two LFS flow rates from the gravimetrical reference flow rate for the undisturbed configuration.

Here, a slight shift of the location of maximal velocities towards -*y* can be observed. For LDA1, the shift was less pronounced. At all lower Reynolds numbers, no noticeable shift could be observed.

Figure 4 shows the deviation of the two LDA systems from the gravimetrical flow rate measurement (the reference) for the undisturbed configuration and the 5 test cases in percent. The deviations were calculated as

$$\Delta Q = 100 * \frac{Q_{\mathrm{LDA}} - Q_{\mathrm{ref}}}{Q_{\mathrm{ref}}}. \qquad (7)$$

The Reynolds numbers were slightly shifted for plotting.

For all individual measurements of the undisturbed case, the maximal deviation from the reference flow rate was 0.21 % at Re = 450*10³ and 60 °C.
All but the measurements at the lowest Reynolds number show a positive deviation from the reference.
The mean absolute deviation between the two LDA systems was below 0.04 %, with a maximum of 0.14 % at Re = 100*10³.

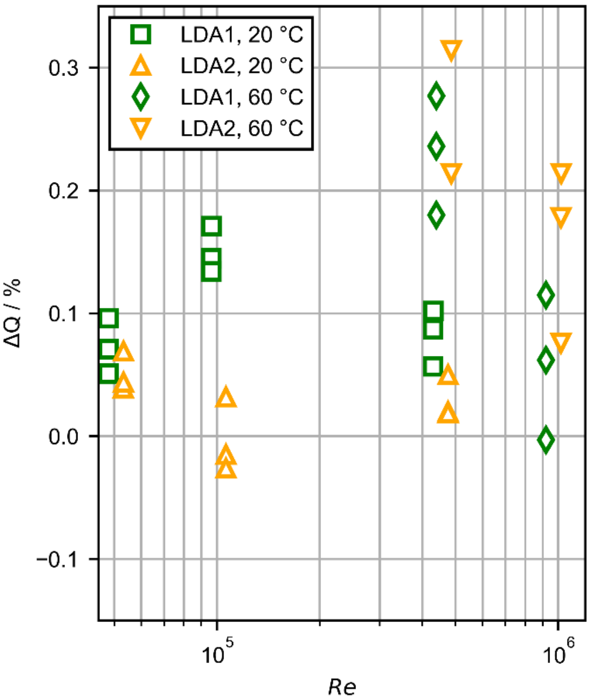

Figure 5: Relative deviations of the two LFS flow rates from the gravimetrical reference flow rate for the disturbed configuration.

The results for the disturbed configuration are presented in Figure 5. At 20 °C, LDA1 exhibited a maximal deviation of 0.17 %, while LDA2 was better than 0.07 %.
At 60 °C however, both systems showed deviations between 0.18 % and 0.31 % for Re = 450*10³. At the highest Reynolds number, deviation from the reference were below 0.21 % for both systems.

For all disturbed measurements, the deviation between the two LDA systems was within 0.16 % and on average at 0.07 %. Compared to the undisturbed case, a higher variance for the test cases at 60 °C was observed.

Due to modifications to the positioning systems, the alignment procedures and for the inclusion of disturbed flow profiles, an up-to-date measurement uncertainty budget for the LFS is currently being developed.
To check for temperature and Reynolds number dependence of the LFS, further measurements across the available temperature range of the test bench must be conducted.

4. Conclusion

The laser optical flow rate standard (LFS) was used to measure the volumetric flow rate of water at 20 and 60 °C and Reynolds numbers between 50*10³ and 945*10³ in a fully developed pipe flow and 6 pipe diameters behind an asymmetrical swirl disturbance generator.
Even in a heavily disturbed flow profile, both independent LDA systems exhibited low deviations from the gravimetrical reference with a mean of 0.12 % and maximal deviations of 0.21 % and 0.31 %, respectively.
This is approximately one order of magnitude below the current measurement uncertainties of flow meters used in power plants, which demonstrates the potential of the LFS as a mobile, laser optical standard for the on-site calibration of industrial flow meters.

References

[1] Furuichi, N., Sato, H., Terao, Y. and Takamotoa, M., “A new calibration facility for water flowrate at high Reynolds number”, Flow Measurement and Instrumentation, **20**, 38-47, 2009.

[2] Mathies, N., “Messunsicherheit einer gravimetrischen Kalt- und Warmwasser-Normalmessanlage für große Volumenströme“, Doctoral dissertation, Technische Universität Berlin, 2005.

[3] Juling, M., “Rückgeführte Volumenstrommessung mittels ortsaufgelöster Laser-Doppler-Anemometrie“, Doctoral dissertation, Technische Universität Berlin, 2016.

[4] Mickan, B., Kramer, R., Hotze, H.J. and Dopheide, D.,"Pigsar The Extended Test Facility and new German National Primary

Standard for High-Pressure Natural Gas", in proceedings of the 5th International Symposium on Fluid Flow Measurement (ISFFM), Arlington, USA, 2002.

[5] Müller, U., Dues, M., Utz, M., Lederer, T. and Büker, O., "Application of Laser Doppler Velocimetry for Monitoring of Measurement Uncertainty of Flow Sensors Under Installation Conditions", in proceedings of “Lasermethoden in der Strömungsmesstechnik” GALA e.V., 2007.

[6] Steinbock, J., “Aufbau und Validierung eines laseroptischen Normal-Durchfluss-Messgeräts für die metrologische Rückführung einer Hochtemperatur-Prüfanlage“, Doctoral dissertation, Technische Universität Berlin, 2017.

[7] Juling, M., Steinbock, J., Kraume, M. and Lederer, T., “LDA volume flow rate standard for water using high spatial resolution LDA for traceable measurements in power plants", in proceedings of FLOMEKO 2016, 2016.

[8] Steinbock, J., Weissenbrunner, A., Juling, M., Lederer and T., Thamsen, P. U., „Uncertainty evaluation for velocity–area methods”, Flow Measurement and Instrumentation, **48**, 51-56, 2016.

[9] Heitmann, F., Juling, M., Steinbock, J. and Kraume, M., “Automated identification of the position and orientation of the LDA measuring volume with respect to flow cross section”, in proceedings of “Lasermethoden in der Strömungsmesstechnik” GALA e.V., 2017.

[10] Steinbock, J. J., Weissenbrunner, A., Juling, M. and Thamsen, P. U., “Correction for the effective measuring position of LDA in circular cross-sections“, in proceedings of “Lasermethoden in der Strömungsmesstechnik” GALA e.V., 2017.

[11] McLaughlin, D. K. and Tiederman, W. G., “Biasing correction for individual realization of laser anemometer measurements in turbulent flows”, The Physics of Fluids, **16**, 2082-2088, 1973.

[12] Tawackolian, K., „Fluiddynamische Auswirkungen auf die Messabweichung von Ultraschall-Durchflussmessgeräten“, Doctoral dissertation, Technische Universität Berlin, 2013.

[13] Turiso, M., Straka, M., Rose, J., Bombis, C. and Hinz, D. F., “The asymmetric swirl disturbance generator: Towards a realistic and reproducible standard”, Flow Measurement and Instrumentation, **60**, 144-154, 2018.